

# Comparison of Two Differential Magnetic-field Probes in Sensitivity

Duan Nie<sup>1,a</sup>, Wenyuan Liu<sup>1,b</sup>, Ruiqi Wang<sup>1,c</sup>, Lei Wang<sup>2,d,\*</sup>

<sup>1</sup>School of Electronic Information and Artificial Intelligence, Shaanxi University of Science and Technology, Xi'an, China

<sup>2</sup>Science and Technology on Reliability Physics and Application of Electronic Component Laboratory, CEPREI, Guangzhou, China

<sup>a</sup>211612062@sust.edu.cn, <sup>b</sup>liuwenyuan@sust.edu.cn, <sup>c</sup>wangruiqi@sust.edu.cn, <sup>d</sup>leiwang@ceprei.com

\*Corresponding author

**Abstract:** As the key element in near-field scanning, electromagnetic probes can locate and diagnose radiation from devices efficiently. To further improve measurement accuracy, different types of probes have been designed to improve performance in terms of bandwidth, spatial resolution, and sensitivity. In this paper, two differential magnetic field probes are designed to enhance sensitivity for near-field scanning. The first probe has a simple U-shaped loop in the detection part. Based on the U-shaped loop as a driven element, the second probe incorporates two identical U-shaped loops as parasitic elements in the detection part to enhance the sensitivity, and the driven loop and two parasitic loops are connected by connected vias separately. The simulated results show that the second differential probe has a higher sensitivity in contrast to the first one.

**Keywords:** Differential probe, Magnetic field, Performance comparison

## 1. Introduction

The rapid advancement of electronic technology has provided great conveniences for individuals and society in many respects. However, electromagnetic radiation from electronic equipment can cause severe electromagnetic interference (EMI), which has a negative effect on equipment performance and even leads to disastrous consequences. To solve the problem effectively, near-field scanning technology is a targeted way to locate and diagnose EMI sources [1].

Near-field scanning technology treats the device under test (DUT) as a "black box" and scans the radiation from the DUT by using electromagnetic probes to analyze and diagnose EMI problems [2]. The design of the electromagnetic probes is the key to near-field scanning technology [3]. A high-performance electromagnetic probe can measure the electromagnetic field distribution near the DUT more accurately. Therefore, more attention has been focused on how to improve the performance of the probes efficiently. A magnetic field probe is designed to develop spatial resolution by miniaturizing the shielded loop coil in the detection part [4]. To widen the frequency, a simple miniature ultra-wideband magnetic field probe is proposed to work in the frequency range of 9 kHz-20 GHz [5]. To enhance the sensitivity, a magnetic field probe is designed to incorporate a Marchand balun and an LC resonant circuit in a differential-loop probe [6].

In this paper, two differential magnetic field probes are proposed and simulated. The first one has a simple U-shaped loop in the detection part. The second one incorporates the simple U-shaped loops as driven elements and two identical U-shaped loops as parasitic elements. The simulated results show that the second probe has a higher sensitivity than the first. The organization of this paper is as follows. In Section 2, the structures of two differential probes are given separately. Section 3 introduces the measurement setup and the characteristics of the probes. Finally, the conclusion is drawn in Section 4.

## 2. The Design of Probe

### 2.1. Probe Structure

Figure 1 shows the three-layer PCB structure of the proposed first differential probe in this paper.

The ground planes with 1.0-oz-thick copper are on the top and bottom layers, and the middle layer is the signal lines plated with 0.5-oz-thick copper. A two-layer stack-up structure consists of two 0.254-mm-thick RO4350B layers. As shown in Figure 2, the differential probe includes a transmission part and a detection part. In the transmission part, there are two striplines and two Sub-Minatures A (SMA) fixed to the probe. There is a simple U-shaped loop in the detection part, and the size of the loop is 0.6 mm × 0.25 mm.

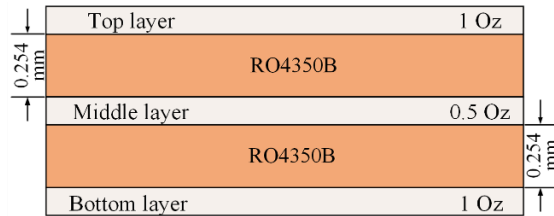


Figure 1: Three-layer PCB structure of the proposed first differential probe.

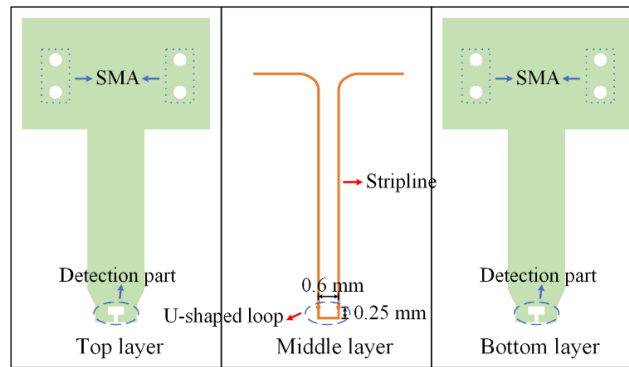


Figure 2: Each layer of the proposed first differential probe's structure.

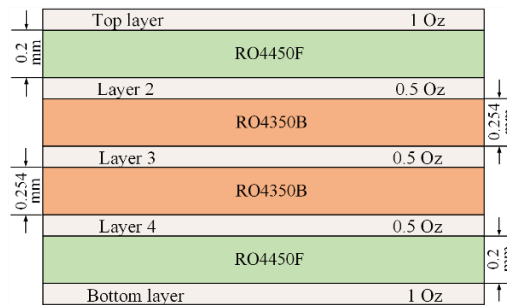


Figure 3: Five-layer PCB structure of the proposed second differential probe.

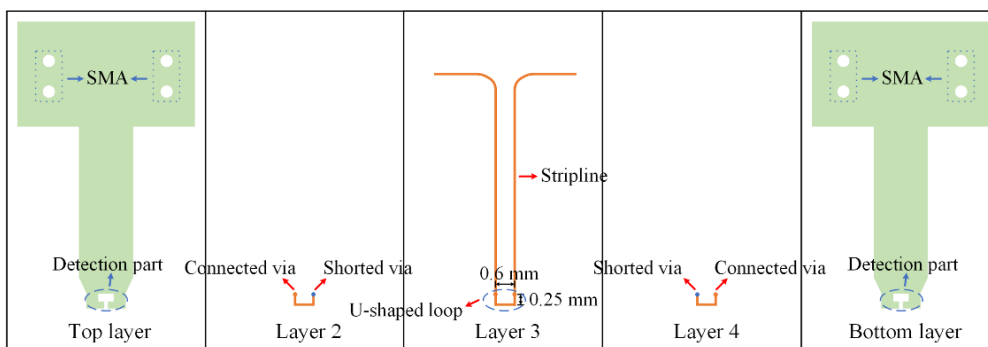


Figure 4: Each layer of the proposed second differential probe's structure.

The five-layer PCB structure of the proposed second differential probe is shown in Figure 3. The top and bottom layers are ground planes plated with 1.0-oz-thick copper, and the signal lines with 0.5-oz-thick copper are on the second, third, and fourth layers. And there is a four-layer stack-up structure, including two 0.254-mm-thick RO4350B layers and two 0.2-mm-thick RO4450F layers. Each layer of the differential probe structure is shown in Figure 4. The transmission part includes striplines with 50-Ω characteristic impedance and two SMAs fixed to the probe. There is a U-shaped loop as a driven element

and two U-shaped loops as parasitic elements in the sensing part. The size of the detection loops is 0.6 mm × 0.25 mm. Two U-shaped loops in the second and fourth layers are separately connected with a U-shaped loop in the third layer by connected vias and connect with ground planes in the top and bottom layers by shorted vias.

### 2.2. U-shaped Loop

The working mechanism of the U-shaped loop is shown in Figure 5, and the two ports of the loop are defined as Port 2 and Port 3 separately. When the U-shaped loop couples to the magnetic field from the microstrip line, the induced voltage at Port 2 is set as  $V_H$ , and the induced voltage at Port 3 is set as  $-V_H$ . Due to the identical length of the two striplines in the loop, the induced voltages at Ports 2 and 3 are both  $V_E$  when the U-shaped loop couples to the electric field.

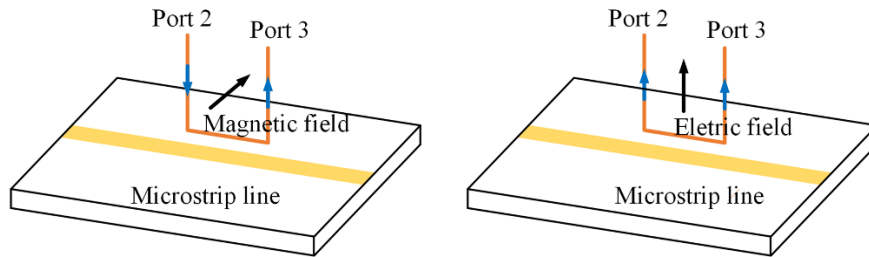


Figure 5: This caption has one line so it is centered.

The total voltages  $V_2$  and  $V_3$  at Ports 2 and 3 can be obtained as follows.

$$\begin{bmatrix} V_2 \\ V_3 \end{bmatrix} = \frac{\sqrt{2}}{2} \begin{bmatrix} 1 & 1 \\ -1 & 1 \end{bmatrix} \begin{bmatrix} V_H \\ V_E \end{bmatrix} \quad (1)$$

By calculating equation (1), the results can be written as

$$\begin{cases} V_H = (V_2 - V_3)/\sqrt{2} \\ V_E = (V_2 + V_3)/\sqrt{2} \end{cases} \quad (2)$$

Where  $V_H$  and  $V_E$  are linearly proportional to magnetic field and electric field. Therefore, the magnetic field and electric field can be obtained by the  $V_H$  and  $V_E$ .

## 3. Characteristics of the Probe

### 3.1. Measurement Setup

Figure 6 shows a measurement setup characterizing probes. The two ends of the microstrip line are connected to a 50 Ω load and Port 1 of a Vector Network Analyzer (VNA) which is the signal source, respectively. Port 2 and Port 3 of the VNA are connected separately to two SMA ends of the probe, which receive signals from Port 1. The differential probe is fixed to a controller, and the movement of the probe is controlled by the software on a personal computer connected to the controller. The tip of the probe is placed directly above the center of the microstrip line, keeping the height at 1 mm.

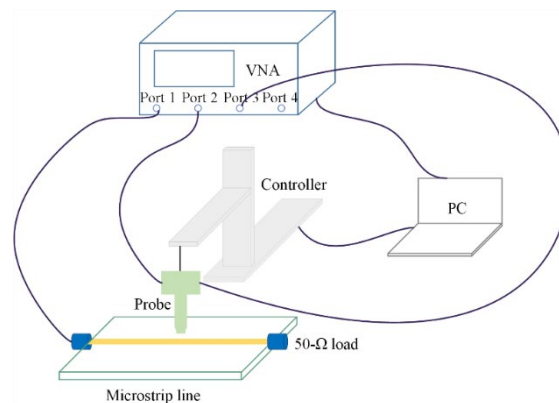


Figure 6: The measurement setup for the Characteristics of probes.

In the measurement, the output of two differential probes can be expressed by the S-parameters:

$$|S_{ds}| = \frac{|S_{31}-S_{21}|}{\sqrt{2}} \quad (3)$$

### 3.2. Simulated Results

The simulated  $|S_{ds}|$  curves of the two differential probes are shown in Figure 7. The frequency response of the second differential probe is higher than that of the first differential probe in the range of 10 MHz-20 GHz. The simulated results show that the second one has a higher sensitivity due to the incorporation of two identical parasitic loops in the detection part.

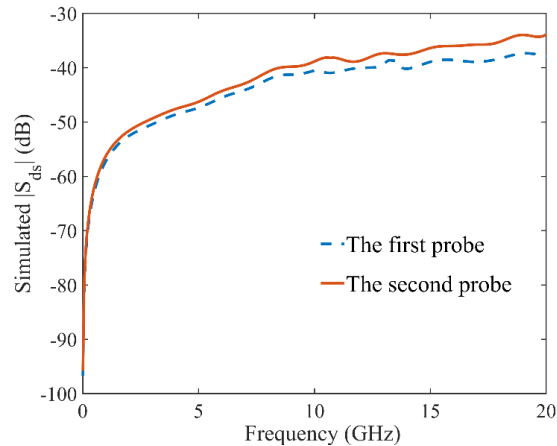


Figure 7: The simulation results of the two differential probes.

### 4. Conclusions

Two differential magnetic field probes are proposed in this paper. The first one is a differential probe with a basic U-shaped loop, and the second one is a differential probe which includes a U-shaped loop as a driven element and two identical U-shaped loops as parasitic elements. According to the simulated results, the second probe has a higher sensitivity than the first.

### References

- [1] J. Shi, M. A. Cracraft, J. Zhang, R. E. DuBroff, and K. Slattery, "Using near-field scanning to predict radiated fields," in *Proc. Int. Symp. Electromagn. Compat*, vol. 1, 2004, pp. 14–18.
- [2] D. Baudry, C. Arcambal, A. Louis, B. Mazari, and P. Eudeline, "Applications of the near-field techniques in EMC investigations," *IEEE Trans. Electromagn. Compat*, vol. 49, no. 3, pp. 485-493, Aug. 2007.
- [3] H. Weng, D. G. Beetner, and R. E. DuBroff, "Prediction of radiated emissions using near-field measurements," *IEEE Trans. Electromagn. Compat*, vol. 53, no. 4, pp. 891–899, Nov. 2011.
- [4] N. Ando et al., "Miniaturized thin-film magnetic field probe with high spatial resolution for LSI chip measurement," in *Proc. Int. Symp. Electromagn. Compat*, vol. 2, Aug. 2004, pp. 357–362.
- [5] Z. Yan, J. Wang, W. Zhang, Y. Wang, and J. Fan, "A simple miniature ultrawideband magnetic field probe design for magnetic nearfield measurements," *IEEE Trans. Antennas Propag.*, vol. 64, no. 12, pp. 5459-5465, Dec. 2016.
- [6] H.-H. Chuang et al., "A magnetic-field resonant probe with enhanced sensitivity for RF interference applications," *IEEE Trans. Electromagn. Compat*, vol. 55, no. 6, pp. 991–998, Dec. 2013.